Fabrication of superhydrophobic/superoleophilic functionalized reduced graphene oxide/polydopamine/PFDT membrane for efficient oil/water separation

Yuanyuan Cheng, Alexandre Barras, Shixiang Lu, Wenguo Xu, Sabine Szunerits, Rabah Boukherroub

Version of Record: https://www.sciencedirect.com/science/article/pii/S1383586619320283
Manuscript_66778fc36358a14d884abbfcaddc05e3

Fabrication of superhydrophobic/superoleophilic functionalized reduced graphene oxide/polydopamine/PFDT membrane for efficient oil/water separation

Yuanyuan Cheng,[a,b] Alexandre Barras,[b] Shixiang Lu,[c] Wenguo Xu,[c] Sabine Szunerits[b] and Rabah Boukherroub[b,*]

[a] *School of Science, China University of Geosciences (Beijing), Beijing 100083, P.R. China*

[b] *Univ. Lille, CNRS, Centrale Lille, ISEN, Univ. Valenciennes, UMR 8520 - IEMN, F-59000 Lille, France*

[c] *School of Chemistry and Chemical Engineering, Beijing Institute of Technology, Beijing 100081, P.R. China*

*To whom correspondence should be addressed:

E-mail: rabah.boukherroub@univ-lille.fr; Fax: +33 362 53 17 01; Tel: +33 362 53 17 24

Abstract

A superhydrophobic/superoleophilic (SS) reduced graphene oxide-polydopamine functionalized with *1H,1H,2H,2H*-perfluorodecanethiol (rGO-PDA-PFDT) membrane was successfully fabricated by a facile and simple two-step method. The surface morphology and chemical composition were thoroughly investigated by scanning electron microscopy (SEM), energy dispersive X-ray (EDX) analysis, UV-vis spectrophotometry, Fourier transform infrared (FT-IR) spectroscopy, Raman spectroscopy, X-ray diffraction (XRD) pattern and X-ray photoelectron spectroscopy (XPS). The wetting properties were assessed using water contact angle (WCA) measurements. The as-prepared rGO-PDA-PFDT membrane displayed a WCA of about 156º, and the water droplet can leave the surface without hysteresis, indicating a stable Cassie-Baxter state. Using the Cassie-Baxter model, we found that approximately 7% serves as the contact area of the water droplet and the solid surface, and the remaining 93% represents the contact area of the water droplet and air. Organic solvents such as chloroform, hexane, toluene, acetone, 1-octane wet completely the surface, indicating superoleophilicity. The superhydrophobic/superoleophilic (SS) membrane was highly stable even in harsh environments such as acid and alkaline media. The rGO-PDA-PFDT was filtered on Whatman filter paper to obtain a membrane and was subsequently applied for oil/water separation. The rGO-PDA-PFDT membrane was able to separate chloroform from water owing to its superhydrophobicity and superoleophilicity. Additionally, the membrane can be reused for 10 repetitive separation cycles without any apparent loss of its performance. These properties are expected to promote the application of the rGO-PDA-PFDT membrane in various environmental processes.

Keywords: *Reduced graphene oxide; Polydopamine; 1H,1H,2H,2H-Perfluorodecanethiol; Superhydrophobicity; Superoleophilicity; Oil/water separation.*

1. Introduction

Graphene, as an allotrope of carbon, has attracted a huge attention of scientists and technologists, because of its outstanding properties such as good chemical stability, high surface area, excellent thermal and electronic conductivity [1-2]. Thus, graphene and its derivatives (graphene oxide and reduced graphene oxide) have been studied separately or in combination with many other materials to produce composite materials with specific properties for potential applications in various fields such as ethanol dehydration, sensing, drug delivery, energy storage and conversion, water purification, etc [3-8].

In nature, mussels can attach to a variety of natural or synthetic substrates and move randomly. Analysis of mussel's byssal proteins revealed that these proteins contain a substantial amount of 3,4-dihdroxy-L-phenylalanine (L-DOPA) and lysine amino acids bearing amino and catechol functional groups [9]. The investigation allowed to identify dopamine (DA) as an interesting synthon for the preparation of adhesive coatings. Indeed, at a weak alkaline pH, DA can self-polymerize in an oxidative process to form an adherent polydopamine (PDA) layer merely on any substrate, demonstrating strong interfacial adhesion ability [10]. Besides its fascinating adhesive property, DA also possesses remarkable reducing properties, which can be used as an eco-friendly and effective reducing agent for the fabrication of multifunctional materials in various research areas [10-13]. The reducing properties of DA have also been applied for the effective reduction of GO and preparation of rGO-polydopamine [14-16] or rGO-DA [17] composites.

Application of polydopamine (PDA) coating on various substrates with the aim to prepare superhydrophobic materials has been investigated in several reports [18-21]. For example, Liu *et al.* prepared compressible and stretchable superhydrophobic polyurethane sponge (PU) using layer-by-layer method [18]. In this approach, PDA was coated on PU, followed by Ag nanoparticles deposition and dodecanethiol functionalization. Oribayo *et al.* fabricated a

superhydrophobic and superoleophilic lignin-based PU foam by grafting polydopamine-reduced graphene oxide (rGO) and octadecylamine (ODA) into the interior part of the foam [21]. Sorption experiments with crude oil, engine oil, kerosene and chloroform showed that the LPU-rGO-ODA foam was an excellent oil sorbent with a sorption capacity of 26-68 times its own weight.

Recently, oil pollution and oil spill have become a global problem [22]. Therefore, there is an urgent need for more effective methods to solve oil contamination. Many methods, including biochemical degradation and physical extraction have been used. In the last years, materials which possess both superhydrophobicity and superoleophilicity have aroused broad attention for oil/water separation [23]. Wang *et al.* formulated a simple, inexpensive, and efficient protocol to achieve a desirable superhydrophobic and superoleophilic surface on conventional filter paper; the superhydrophobic filter paper showed nanostructured morphology and demonstrated great separation efficiency (up to 99.4%) for water/oil mixtures [23]. Suhas *et al.* prepared a graphene loaded polymer composites of chitosan and poly (vinyl pyrrolidone) for pervaporation (PV) dehydration of ethanol [24]. Although many materials have been used for reducing oil contaminant, there are still much challenges to overcome, such as high cost, poor recyclability, and so on. Novel materials that are cost-effective and easy-to-prepare are still highly in demand for efficient oil/water separation.

In this study, a superhydrophobic and superoleophilic reduced graphene oxide coated with polydopamine chemically functionalized with low surface free energy *1H,1H,2H,2H*-perfluorodecanethiol (PFDT), rGO-PDA-PFDT, composite was fabricated successfully by a facile and a simple two-step immersion method. The rGO-PDA-PFDT was vacuum filtered through a Whatman filter paper to produce a superhydrophobic/superoleophilic rGO-PDA-PFDT membrane. The superhydrophobic property was stable in harsh conditions with no apparent evolution after 24 h immersion of the membrane in acidic and alkaline media. The

rGO-PDA-PFDT membrane was capable of separating immiscible organic solvent/water mixtures with high efficiency.

2. Experimental section

2.1. Materials

All chemicals were reagent grade or higher and were used as received unless otherwise specified. Phosphate buffered saline (PBS), dopamine hydrochloride (DA, $C_8H_{11}NO_2 \cdot HCl$), *1H,1H,2H,2H*-perfluorodecanethiol (PFDT, $C_{10}H_5F_{17}S$, 97%), sodium hydroxide (NaOH, ≥98%), hydrochloric acid (HCl, ~37%), ethanol (CH_3CH_2OH, 95%), and the Whatman qualitative paper (grade 1, diameter 25 mm) were purchased from Sigma-Aldrich. The water used throughout the experiments was purified with a Milli-Q system from Millipore Co.

GO was prepared from native graphitic flakes according to the modified Hummer's and Offeman method. The detailed experimental conditions can be found in our previous report [25].

Methylene Blue (MB, $C_{16}H_{18}ClN_3S \cdot 3H_2O$) and Rhodamine B (RhB, $C_{28}H_{31}ClN_2O_3$) were purchased from Sigma-Aldrich and used to color the HCl solution (pH 1) and NaOH solution (pH 14), respectively. Methylene Blue was also used to color the chloroform for clear observation of the oil/water separation experiment.

2.2. Fabrication of rGO-PDA-PFDT porous membrane

Individual graphene oxide (GO) sheets were exfoliated from graphite oxide (3 mg) in PBS buffer solution (10 mL) with the help of ultrasound for 2 h. Then, NaOH aqueous solution (0.1 mol/L) was added into the suspension dropwise and the pH was adjusted to 8.5. Nitrogen was bubbled into the solution steadily for 20 min to remove dissolved oxygen in the solution. After addition of dopamine (DA, 3 mg), the colloidal suspension was sealed quickly. The mixed suspension was further stirred at room temperature for 3 h, resulting in the formation of

rGO-PDA composite. In this process, we can clearly see that the color of the suspension changed from light brown to deep brown, as shown in **Figure 1**. The resulting deep brown precipitate was separated from the aqueous supernatant by centrifugation at 6000 rpm for 30 min. Without drying, absolute ethanol (10 mL) was added into the rGO-PDA suspension solution and subjected to ultrasonication for 30 min to achieve a homogeneous dispersion. Then, *1H,1H,2H,2H*-perfluorodecanethiol (PFDT, 25 μL) was added into the ethanol solution. The mixed solution was reacted at room temperature for 24 h with magnetic stirring. After that, the color of the solution became darker.

The rGO-PDA-PFDT membrane was fabricated by vacuum filtration of the mixed suspension through a Whatman filter paper, followed by air drying in the oven at 50°C for 1 h and peeling off the filter paper. For comparison, pristine GO and rGO-PDA membranes were fabricated by filtering a GO or rGO-PDA dispersion similar to the above described approach, respectively.

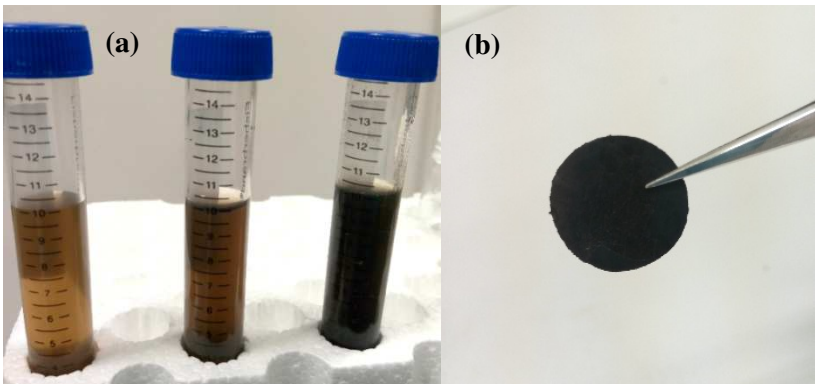

Figure 1. (a): The digital photos (from left to right) of GO aqueous solution (light brown), GO aqueous solution + DA for 3 h (deep brown), rGO-PDA ethanol solution + PFDT for 24 h (black), (b): as-prepared rGO-PDA-PFDT membrane peeling off the filter paper.

2.3. Characterization

Scanning electron microscope (SEM)

Scanning electron microscopy (SEM) images and energy dispersive X-ray (EDX) spectra of the samples were obtained using an FEI Nova NanoSEM 450 scanning electron microscope

with FEG (field emission gun, Schottky type) system equipped with an energy dispersive X-ray analyzer at an accelerating voltage of 20 kV.

UV/Vis spectrophotometry

Absorption spectra were recorded by using a Perkin-Elmer Lambda UV/Vis 950 spectrophotometer in plastic cuvettes with an optical path of 10 mm. The wavelength range was 200-600 nm.

Fourier transform infrared spectroscopy (FTIR)

Transmission FTIR spectra were recorded using a Perkin-Elmer Spectrum One FTIR spectrometer with a resolution of 4 cm^{-1} using KBr pellets. Dried powder (1 mg) was mixed with KBr powder (100 mg) in an agate mortar. The mixture was pressed into a pellet under 10 tons load for 2-4 min, and the spectrum was recorded immediately. Thirty-six accumulative scans were collected. The signal from a pure KBr pellet was subtracted as a background.

Raman spectroscopy

Micro-Raman spectroscopy measurements were performed on a Horiba Jobin Yvon LabRam HR Micro-Raman system combined with a 473 nm laser diode as excitation source. Visible light was focused by a 100× objective. The scattered light was collected by the same objective in backscattering configuration dispersed by a 1800 mm focal length monochromator and detected by CCD.

X-ray powder diffraction (XRD)

The crystal structure was determined by using an X-ray powder diffractometer (XRD, D8 Advance, Bruker, Germany) with Cu Kα radiation at a continuous scanning mode (40 kV, 40 mA, and $\lambda = 0.15418$ nm) and scanning rate of $3° \ min^{-1}$.

X-ray photoelectron spectroscopy (XPS)

XPS measurements were performed with an ESCALAB 220 XL spectrometer from Vacuum Generators featuring a monochromatic Al Kα X-ray source (1486.6 eV) and a spherical

energy analyzer operated in the CAE (constant analyzer energy) mode (CAE = 100 eV for survey spectra and CAE = 40 eV for high-resolution spectra), using the electromagnetic lens mode. The detection angle of the photoelectrons is 30°, as referenced to the sample surface.

Contact angle measurements

Water contact angles were measured using deionized water. We used a remote computer-controlled goniometer system (Digi-drop from GBX, Bourg-de-Peage, France) for measuring the contact angles. The accuracy is ±1°. All measurements were conducted in an ambient atmosphere at room temperature.

3. Results and discussion

3.1. Preparation of rGO-PDA-PFDT composite

Superhydrophobic and superoleophilic rGO-PDA-PFDT composite was fabricated successfully by a facile and a simple two-step immersion method, as shown in **Scheme 1**. Graphene oxide (GO) sheets were dispersed in PBS buffer solution and the pH was adjusted to 8.5 by NaOH solution. Then, dopamine was added into this suspension, resulting in the formation of rGO-PDA composite. After centrifugation, *1H,1H,2H,2H*-perfluorodecanethiol (PFDT) was added into the rGO-PDA ethanol solution to produce rGO-PDA-PFDT composite. Then vacuum filtration through a Whatman filter paper was applied to obtain a membrane. The wetting properties, morphology, and chemical composition of the membrane were characterized using various techniques.

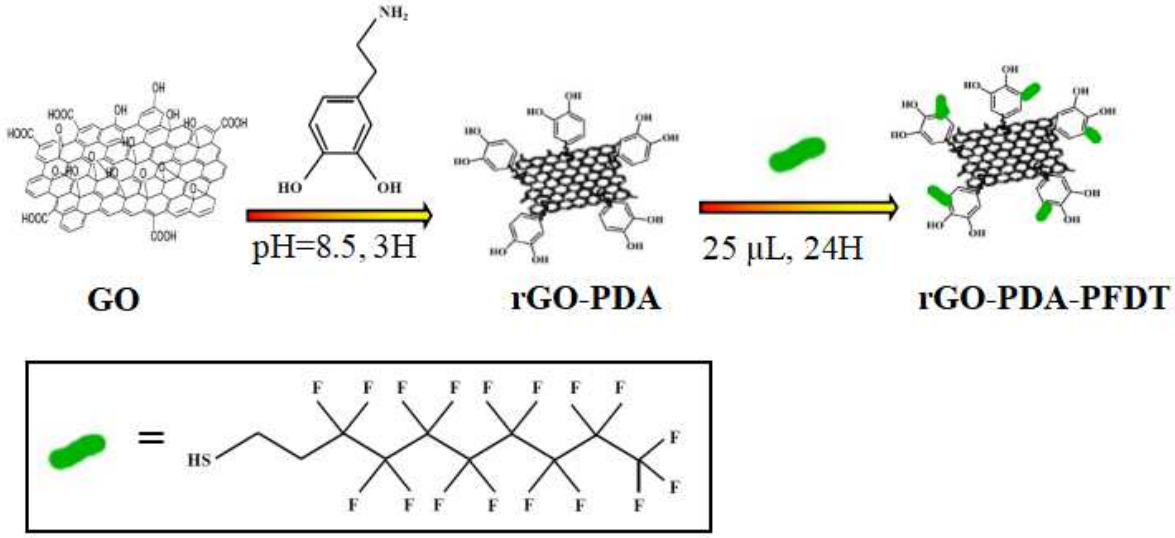

Scheme 1. Schematic illustration of the preparation of rGO-PDA-PFDT.

3.2. Wettability

Figure 2 depicts the images of static water contact angles (SWCA) on the GO, rGO-PDA and rGO-PDA-PFDT membrane surfaces, respectively, which clearly demonstrate the changes of wettability. The SWCA of GO membrane is approximately 75º, indicating the hydrophilic character of the membrane. After reaction with DA for 3 h, the SWCA decreases to 10º, in agreement with polydopamine formation. Indeed, polydopamine comprises many polar groups that confer a hydrophilic character to the membrane. Interestingly, after treatment with PFDT for 24 h, the wetting properties of the rGO-PDA-PFDT membrane successfully changed to superhydrophobicity with a SWCA of 156º. This can be attributed to the presence of low surface energy groups (-CF_2 and -CF_3) in the PFDT molecule.

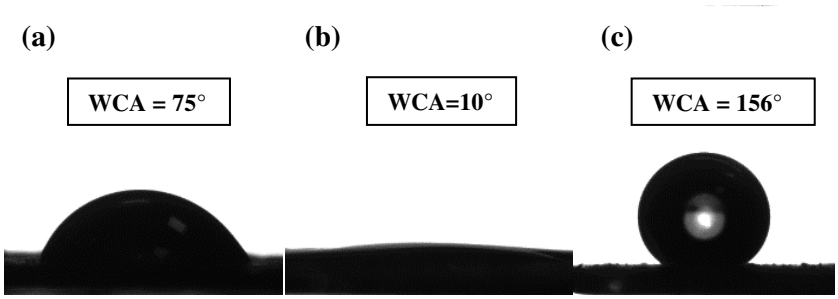

Figure 2. The static water contact angles (SWCA) of GO (a), rGO-PDA (b), and rGO-PDA-PFDT membranes (c).

Next, we investigated the anti-sticking property of the rGO-PDA-PFDT membrane on a horizontal surface, as shown in **Figure 3** and **Video S1**. By moving down and up the needle at a speed of 0.5 mm/s, the water droplet at the end of the needle can touch and leave the membrane simultaneously. We found that the water droplet always kept a spherical or contorted spherical shape, instead of spreading on the surface. Additionally, the droplet leaves the surface without hysteresis, suggesting the anti-sticking property of the membrane. The anti-sticking property of the rGO-PDA-PFDT superhydrophobic membrane may facilitate its potential and practical applications such as water repellency, self-cleaning and anti-icing.

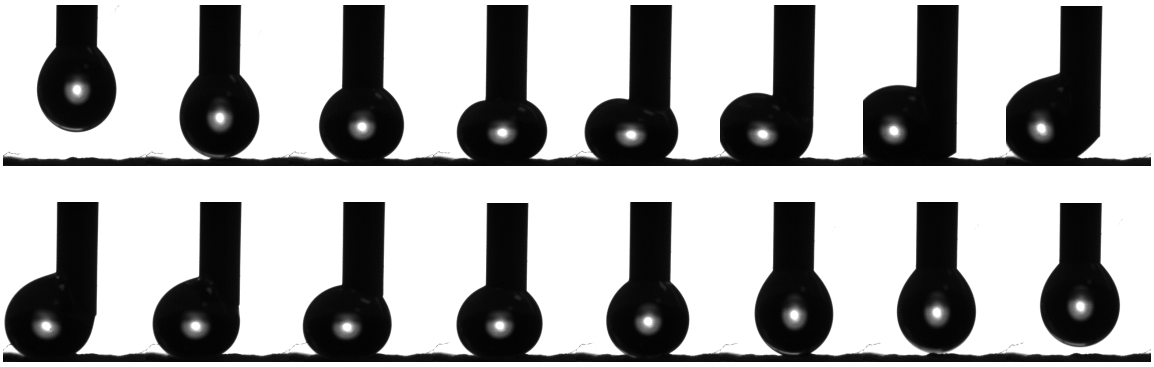

Figure 3. Successive snapshots of 8 μL water droplet on the superhydrophobic rGO-PDA-PFDT membrane.

3.3. Theoretical explanation of the wettability

In general, there are two models to describe the superhydrophobicity: (1) In the Wenzel model [26], the liquid can totally wet the solid surface and no gas bubbles between the liquid and the solid surface can be found. (2) The Cassie-Baxter [27] model suggests that there are gas bubbles residing between the liquid and the solid and the surface cannot be totally wetted. The Wenzel model describes the wetted surface by the following equation:

$$\text{Cos } \theta^* = r \text{ Cos } \theta \qquad (1)$$

where θ^* is the Wenzel CA, θ is the CA of the smooth surface, and r is the roughness ratio, defined as the ratio of the true surface area of the structure to its projection area.

In the Cassie-Baxter model, the non-uniform wetting is described by the following equation:

$$\text{Cos}\ \theta^* = f_1\ \text{Cos}\ \theta - f_2 \qquad (2)$$

where θ^* is the Cassie-Baxter CA, θ is the CA of the smooth surface, f_1 is the ratio of the solid and liquid interface to the projection area, f_2 is the ratio of the solid and gas interface to the projection area, and $f_1 + f_2 = 1$.

The water droplet on the surface of rGO-PDA-PFDT membrane exhibits a completely superhydrophobic character; the droplet can stay on the membrane without adhesion and can leave the membrane without hysteresis, according to the Cassie-Baxter model [27], indicating that microscopic pockets of air may be trapped below the water droplet. Therefore, the Cassie-Baxter state is considered. Given that $\theta^* = 156^\circ$ and $\theta = 75^\circ$, f_1 and f_2 are estimated as 0.07 and 0.93, respectively. These data indicate that when a water droplet is placed on a superhydrophobic surface, approximately 7% serves as the contact area of the water droplet and the solid surface, and the remaining 93% represents the contact area of the water droplet and air. Consequently, the liquid droplet is non-sticky to the surface and the adhesion between droplet and surface is low.

3.4. Surface morphology

Figure 4 displays the SEM images of GO, rGO-PDA and rGO-PDA-PFDT membranes, clearly revealing different surface morphologies. In **Fig. 4(a)**, the GO membrane displays a relatively smooth surface without other apparent impurities. From the magnification in **Fig. 4(b)**, the GO layer is relatively thin. After GO reaction with dopamine for 3 h, the surface morphology is slightly altered (**Fig. 4(c)**). From the magnification in **Fig. 4(d)**, we can clearly see that the rGO layers are encapsulated by a thin membrane. The WCA of the surface

changes from 75º to 10º (**Fig. 2**). This is in accordance with the Wenzel theory [26], suggesting that the hydrophilicity of a surface is enhanced with increasing its roughness. However, after subsequent immersion in PFDT solution for 24 h, abundant clusters and embossments appeared with different sizes and various shapes (**Fig. 4(e, f)**), implying that PFDT possesses hydrophobic ability, and the WCA of the surface increased to 156º (**Fig. 2**).

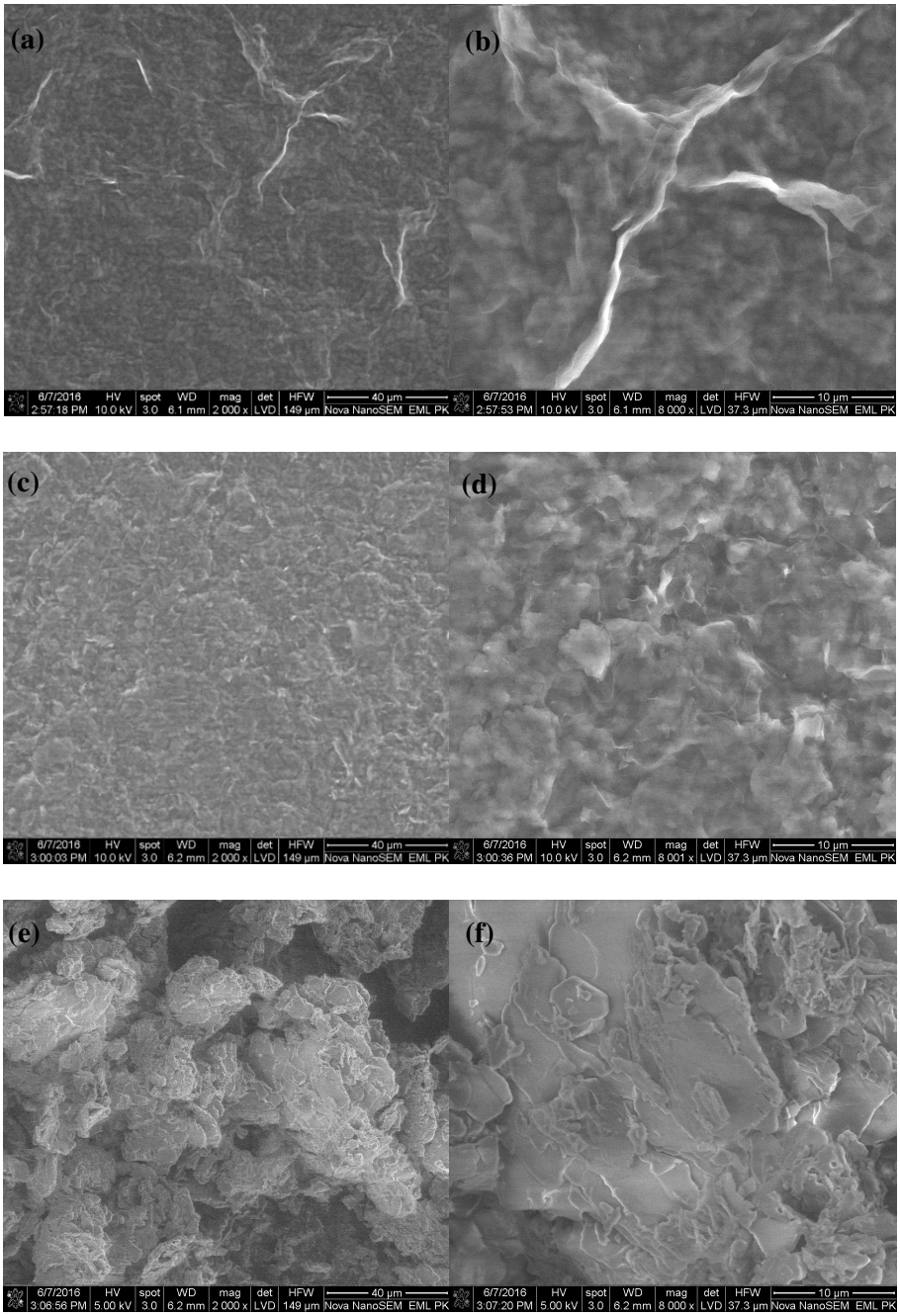

Figure 4. SEM images of GO (a and b), rGO-PDA (c and d) and rGO-PDA-PFDT (e and f) membranes.

3.5. Surface composition

3.5.1. EDX analysis

In order to confirm the surface elemental composition, EDX analysis was performed on the different surfaces. The EDX spectrum of GO membrane consists mainly of carbon (60.79 at.%) and oxygen (38.76 at.%), in good agreement with the chemical composition of GO (**Fig. 5(a)**). Meanwhile, the existence of low concentrations of S and Mn elements can be attributed to H_2SO_4 and $KMnO_4$ introduced during severe oxidation processes used in the modified Hummer's and Offeman method. **Fig. 5(b)** exhibits the EDX spectrum of rGO-PDA membrane. It comprises peaks due to carbon (60.58 at.%) and oxygen (34.42 at.%), and additional peaks due to Na, P, Cl, K elements, which can be ascribed to main salts from PBS that have not been fully removed from the membrane. Subsequent functionalization of rGO/PDA with PFDT obviously introduced a large amount of fluorine (49.47 at.%) and sulfur (3.55 at.%), indicating successful PFDT grafting onto the PDA layer (**Fig. 5(c)**).

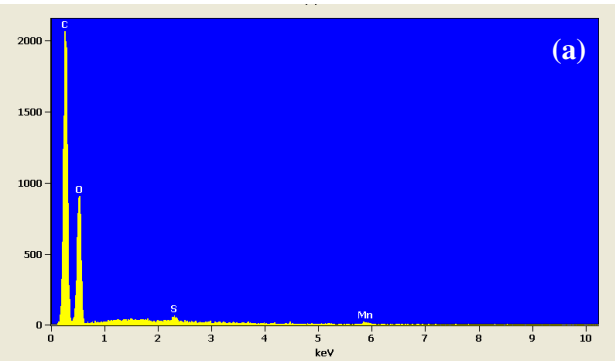

Element Line	Weight %	Weight % Error	Atom %	Atom % Error
C K	53.25	± 0.45	60.79	± 0.51
O K	45.23	± 0.63	38.76	± 0.54
S K	0.42	± 0.04	0.18	± 0.02
Mn K	1.10	± 0.16	0.27	± 0.04
Total	100.00		100.00	

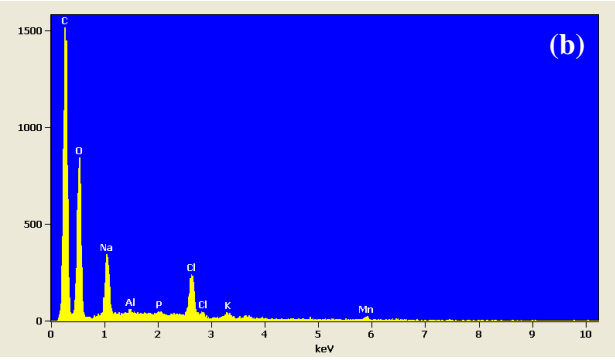

Element Line	Weight %	Weight % Error	Atom %	Atom % Error
C K	51.17	± 0.49	60.58	± 0.57
O K	38.73	± 0.57	34.42	± 0.50
Na K	4.94	± 0.11	3.05	± 0.07
Al K	0.17	± 0.03	0.09	± 0.02
P K	0.23	± 0.03	0.11	± 0.02
Cl K	3.20	± 0.11	1.28	± 0.05
K K	0.55	± 0.09	0.20	± 0.03
Mn K	1.01	± 0.15	0.26	± 0.04
Total	100.00		100.00	

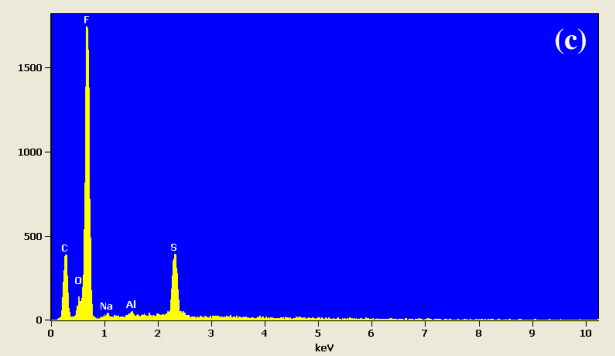

Element Line	Weight %	Weight % Error	Atom %	Atom % Error
C K	30.92	± 0.53	42.27	± 0.72
O K	4.01	± 0.46	4.11	± 0.47
F K	57.25	± 0.54	49.47	± 0.46
Na K	0.57	± 0.10	0.41	± 0.07
Al K	0.31	± 0.04	0.19	± 0.02
S K	6.94	± 0.15	3.55	± 0.08
Total	100.00		100.00	

Figure 5. EDX spectra of GO (a), rGO-PDA (b) and rGO-PDA-PFDT (c) membranes.

3.5.2. UV-vis analysis

UV-vis absorption was used to identify the presence of a conjugated system in the graphenic-based membranes. **Figure 6** illustrates the UV-vis absorption spectra of GO and rGO-PDA in PBS solution, and rGO-PDA-PFDT in absolute ethanol. For GO, a characteristic absorbance peak at about 230 nm and a shoulder peak at around 290-300 nm, which can be assigned to the π-π* transition of C=C and n→π* transition of the carbonyl groups, respectively, are observed (**Fig. 6a**). After GO reaction with dopamine (DA), the UV-vis absorption spectrum displays a characteristic absorption of catechols in polydopamine at 280 nm [28], indicating PDA coating on the GO surface (**Fig. 6b**). This result is comparable to that reported by Zhong *et al.* [29]. Subsequent surface functionalization with *1H,1H,2H,2H*-perfluorodecanethiol (PFDT) shows an obvious absorption peak at about 269 nm, which is a clear indication of partial reduction of GO to rGO during PDA formation and PFDT modification (**Fig. 6c**). This observation is consistent with the restoration of the sp^2 structure in rGO and in good agreement with previous studies on GO functionalization with catechol moieties [24, 28].

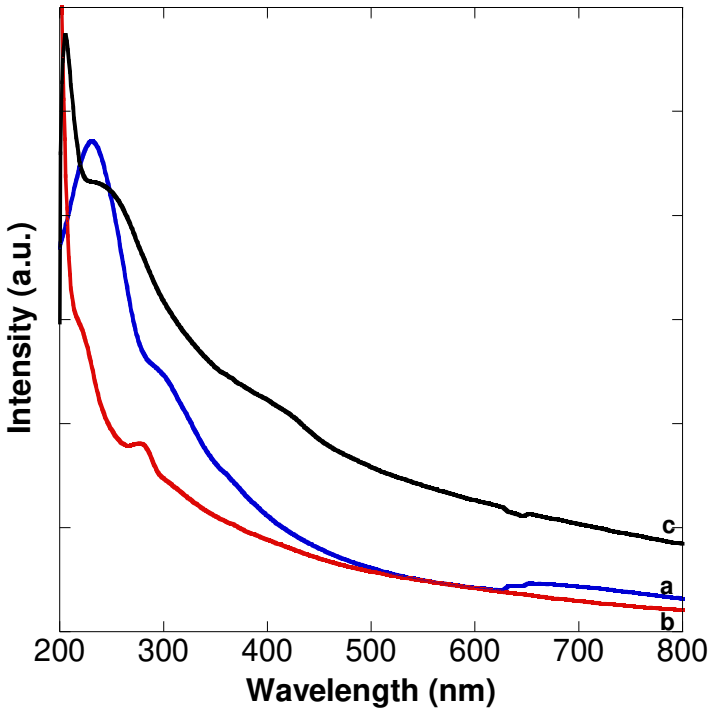

Figure 6. UV-vis absorption spectra of aqueous dispersion of GO (a, blue line), rGO-PDA (b, red line) and ethanol dispersion of rGO-PDA-PFDT (c, black line).

3.5.3. FT-IR analysis

The chemical composition and changes of functional groups that occurred during GO functionalization with dopamine and subsequent modification with PFDT have been detected by Fourier transform infrared (FTIR) spectroscopy (**Fig. 7**). The FTIR spectrum of the starting GO depicts the following characteristic peaks: a broad and intense O-H stretching peak at 3389 cm^{-1}, C=O stretching vibration of carboxyl groups at 1736 cm^{-1}, aromatic C=C stretching vibration at 1621 cm^{-1}, O-H deformation vibration at 1351 cm^{-1}, C-OH stretching at 1225 cm^{-1}, and C-O stretching at 1054 cm^{-1} (**Fig. 7a**) [29-31].

After dopamine self-polymerization on the GO surface, the disappearance of the typical C=O peak at 1736 cm^{-1} compared to pristine GO strongly suggests the partial reduction of GO to rGO. Two new features at 1653 and 1559 cm^{-1} assigned to the vibrations of C=C ring and C=N ring stretching modes, respectively, confirm the presence of aromatic amine species [32].

The strong peak at 1384 cm^{-1} is attributed to indole ring CNC stretching modes, indicating the presence of indole features in PDA [33]. The broad peak in the 3700-3300 cm^{-1} range can be assigned to the vibration of N-H and O-H stretching modes [34, 35]. The shift can indicate a loss of primary amine groups (peaks expected at ≈3500 cm^{-1} for the vibration of N-H asymmetric and 3400 cm^{-1} for the vibration of N-H symmetric modes) and generation of secondary amines (peak at ≈3330 cm^{-1}), as is expected in the formation of PDA. Furthermore, the broad peak at about 3315 cm^{-1} is slightly red-shifted, indicating the generation of PDA (**Fig. 7b**).

Upon functionalization with the fluorinated PFDT compound, the stretching vibration of -OH groups at about 3380 cm^{-1} was further reduced and became almost invisible. Additionally, two characteristic peaks corresponding to C-S-C and -C-F bonds of the PFDT molecule appear at 1202 and 1148 cm^{-1}, respectively, indicating PDA functionalization with PFDT molecules [19]. Hence, treatment with low energy molecules such as PFDT can be used to endow a hydrophobic property of the sample by removing residual -OH groups from GO surface.

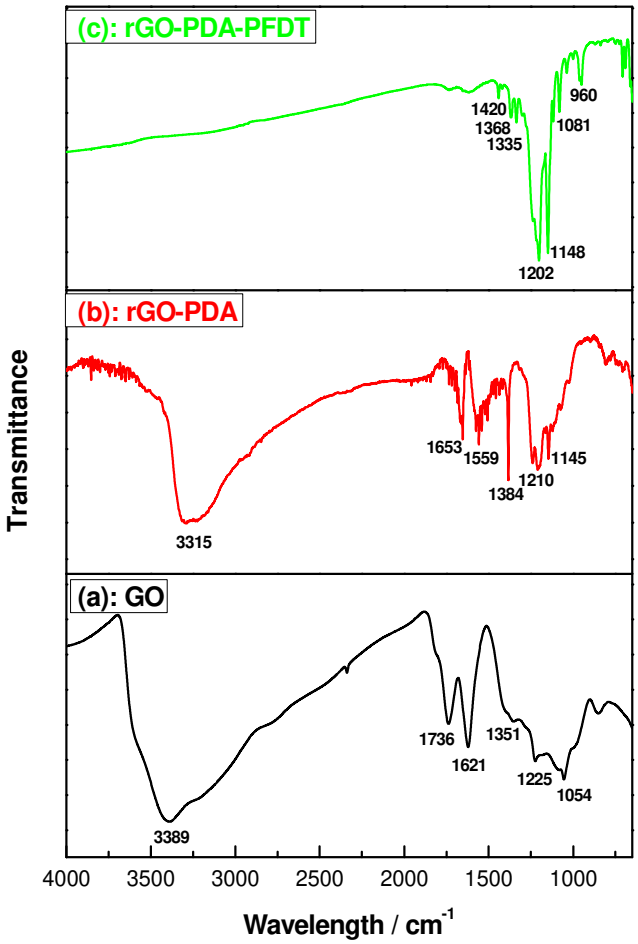

Figure 7. FT-IR spectra of GO (**a**, black line), rGO-PDA (**b**, red line) and rGO-PDA-PFDT powders (**c**, green line).

3.5.4. Raman analysis

Raman scattering is a useful tool for characterizing the structural properties of graphene-based materials. **Figure 8** depicts the Raman spectra of GO, rGO-PDA and rGO-PDA-PFDT membranes; the main features of the graphene-based materials are a D band at 1356 cm^{-1}, a G band at 1589 cm^{-1}, and a 2D band at around 2700 cm^{-1} [36]. The ratios of the intensities of the D and G bands (I_D/I_G) are 0.929 for GO, 0.894 for rGO-PDA and 0.881 for rGO-PDA-PFDT, indicating the decrease of defects and disorders after successive modification of GO with

PDA and PFDT. After GO reduction with dopamine, more sp^2 carbon network has been restored, while most sp^3 components have been removed.

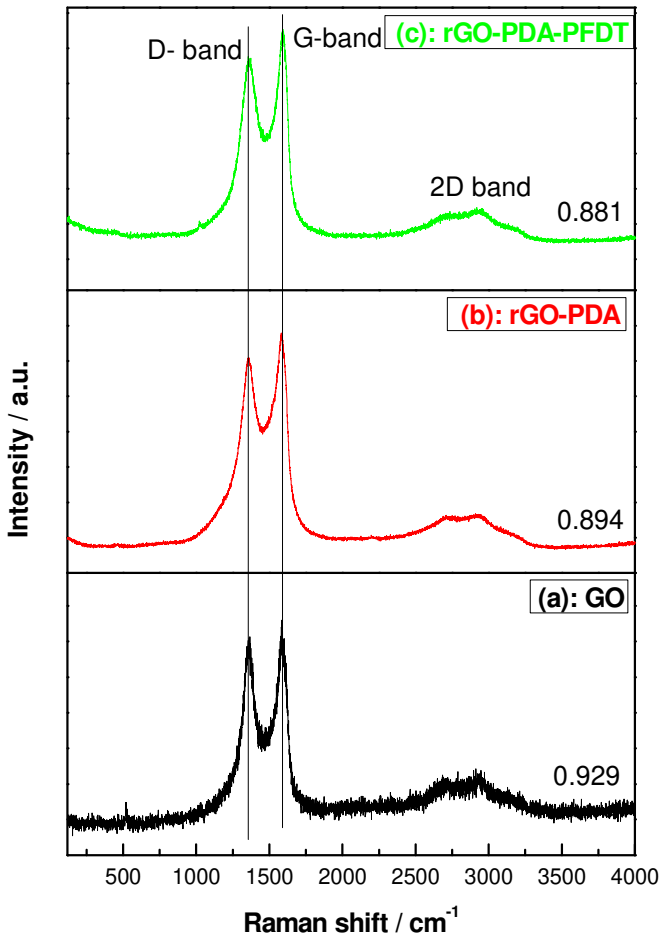

Figure 8. Raman spectra of GO (**a**, black line), rGO-PDA (**b**, red line) and rGO-PDA-PFDT membranes (**c**, green line).

3.5.5. XRD analysis

To further illustrate the surface composition changes upon PDA formation and its subsequent modification with PFDT molecules, XRD spectra are recorded (**Fig. 9**). The symbols of *, # and ° represent the peaks of $CF_{1.1}$, $C_{2.9}F$ and $C_{15}S_4$, respectively. As a comparison, the XRD patterns of bare GO and rGO-PDA powder are also recorded and shown in **Fig. 9(a, b)**, respectively. In **Fig. 9a**, the strong sharp peak at 2θ of 11.50° is

assigned to the diffraction from (001) planes of GO; the broad peaks at *2θ* of 19.24°, 30.61° and 42.43° are attributed to the π→π stacking interactions of the aromatic rings [37]. After reaction with dopamine, the main diffraction peak of GO decreased while shifting to a smaller diffraction angle, indicating a gradual increase of the gap between the GO sheets owing to the insertion of dopamine (**Fig. 9b**). The existence of the peak at *2θ* of 8.32° indicates that not all of GO has been reduced to rGO, and there are still some oxidized domains in the rGO sheets.

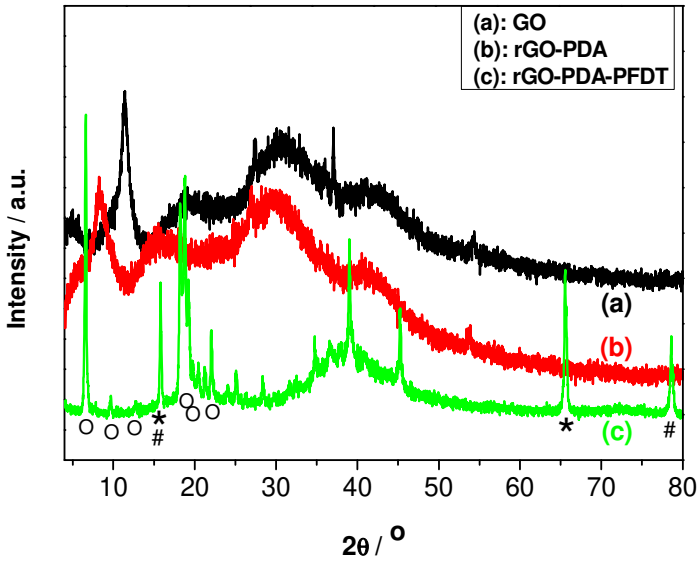

Figure 9. XRD patterns of GO (**a**, black line), rGO-PDA (**b**, red line) and rGO-PDA-PFDT powders (**c**, green line).

For rGO-PDA-PFDT, many sharp peaks appear in the XRD pattern, suggesting that crystallinity exists within the material (**Fig. 9c**). For example, the peaks at *2θ* of 15.37° and 64.93° can be assigned to the diffraction peaks of $CF_{1.1}$ (001) and $CF_{1.1}$ (004), respectively (JCPDS card no. 30-0476). The peaks at *2θ* of 15.54° and 78.00° can be attributed to the diffraction peaks of $C_{2.9}F$ (002) and $C_{2.9}F$ (110), respectively (JCPDS card no. 49-1409). The peaks in the 5-23° range can be ascribed to $C_{15}S_4$ (110), $C_{15}S_4$ (200), $C_{15}S_4$ (021), $C_{15}S_4$ (330), $C_{15}S_4$ (311) and $C_{15}S_4$ (-422) at *2θ* of 6.20°, 9.10°, 12.33°,18.60°, 19.41° and 22.20°,

respectively (JCPDS card no. 65-1164) from left to right. Other peaks can be attributed to carbon crystals. The existence of many sharp peaks suggests that the rGO-PDA-PFDT is crystalline.

3.5.6. X-ray photoelectron spectroscopy (XPS) analysis

To further gain more insights on the elemental composition of the membrane and to obtain detailed information on the chemical states of different elements, XPS measurements were performed. **Fig. 10a** displays the general survey spectra of rGO-PDA and rGO-PDA-PFDT membranes. The XPS survey spectrum of rGO-PDA consists mainly of C_{1s}, N_{1s} and O_{1s} along with small contribution from Na_{1s} and Cl_{2p} from PBS, in agreement with the chemical composition of the membrane. After functionalization of the PDA coating with PFDT, additional peaks due to S_{2p} and F_{1s} can be seen in the XPS survey spectrum of rGO-PDA-PFDT, confirming the successful incorporation of PFDT moieties in the PDA layer.

Typical high resolution scans of C_{1s}, S_{2p} and F_{1s} are depicted in **Fig. 10b-e**, respectively. The high resolution XPS spectrum of the C_{1s} region of rGO-PDA can be fitted with two components at 284.2 and 286.3 eV due to C-C and C-O/C-N bonds, respectively (**Fig. 10b**). After PFDT grafting on rGO-PDA, a significant change can be seen in the high resolution XPS spectrum of the C_{1s}, with a most notable decrease of the C-O/C-N component at 285.7 eV. The spectrum can be deconvoluted into four main components at 284.2, 285.7, 291.3 and 293.4 eV (**Fig. 10c**). The two new peaks at 291.3 and 293.4 eV are attributed to C-F bond from CF_2 and CF_3, respectively, in accordance with PFDT grafting on the PDA layer [38, 39].

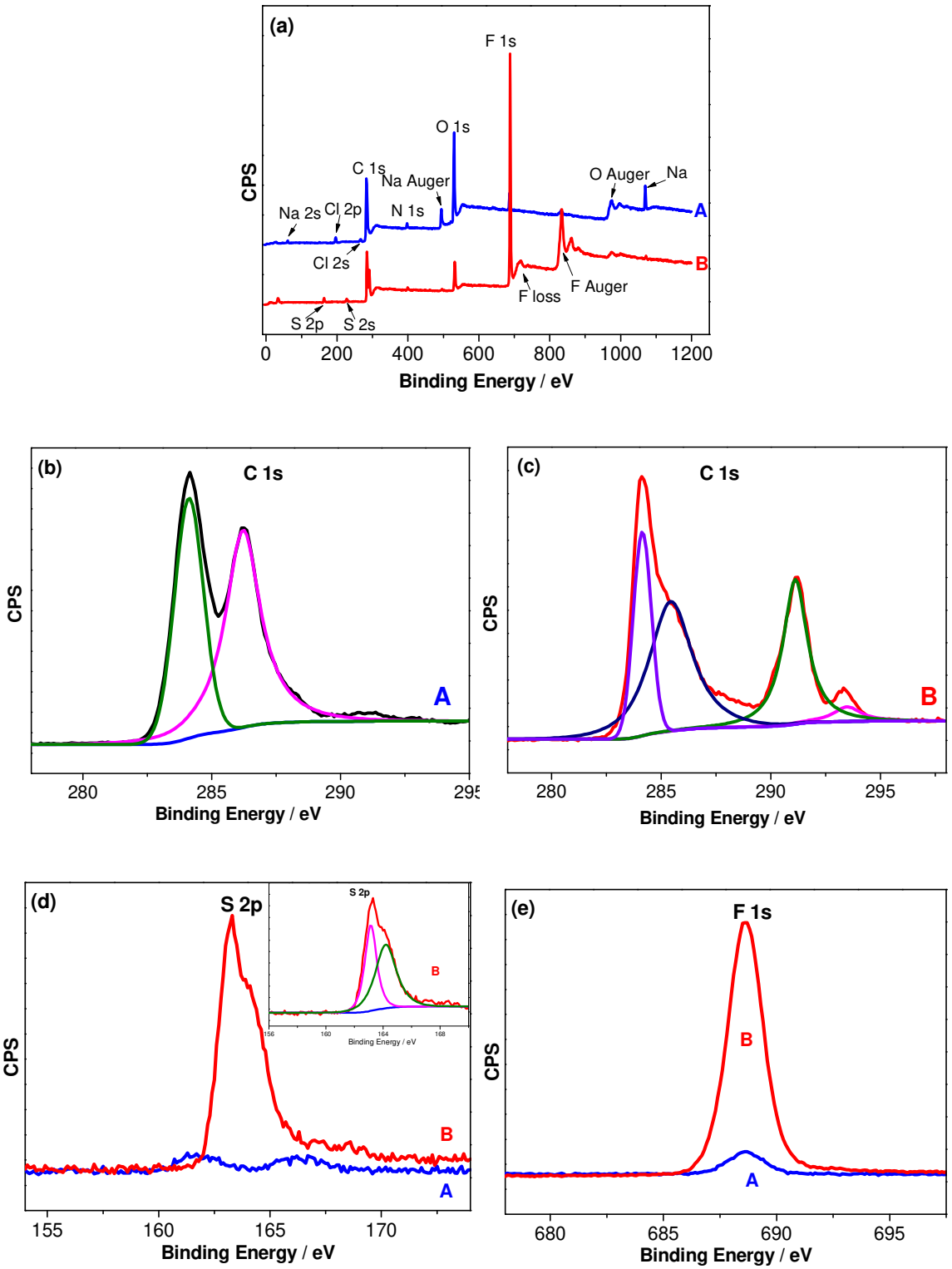

Figure 10. XPS spectra: (a) the survey spectra, (b) fitted curve of C_{1s} region of sample A, (c) fitted curve of C_{1s} region for sample B, (d) S_{2p} region, and the inset is fitted curve of sample B, (e) F_{1s} region; (A) rGO-PDA (blue line), (B) rGO-PDA-PFDT (red line).

The high resolution XPS scans of the O_{1s} region of rGO-PDA and rGO-PDA-PFDT are displayed in **Fig. S1a**. The O_{1s} spectrum of rGO-PDA exhibits an asymmetric peak that can be deconvoluted into two components with binding energies at 529.6 and 530.8 eV, which can be attributed to the O-H and O-C bonds, respectively. After grafting PFDT on the PDA layer, the intensity of the peaks decreased distinctly, while their binding energies are barely changed, indicating a significant decrease of the oxygen content.

The XPS wide scan of the N_{1s} is depicted in **Fig. S1b**. In curve A, the N_{1s} peak appeared at about 399.81 eV, which can be ascribed to the amine groups in the heterocycle of PDA, suggesting that no free-end amine groups remain on the surface, and that PDA had been successfully coated on reduced graphene oxide [40, 41]. After modification with PFDT (curve B), the N_{1s} peak at 399.81 eV is still visible, but the intensity of the peaks decreased distinctly. Given that XPS is a surface sensitive tool, PFDT immobilization on the PDA surface weakens the intensity of underneath nitrogen.

The XPS wide scans of the S_{2p} and F_{1s} are displayed in **Fig. 10d** and **Fig. 10e**, respectively. Both spectra indicate that before PFDT grafting (curve A), there were almost no peaks due to S and F. These peaks became apparent after PDA functionalization with PFDT, in good agreement with the chemical transformation that has occurred on the surface. While the F_{1s} spectrum exhibits a symmetrical peak at 688.62 eV, the S_{2p} spectrum can be deconvoluted into two bands at 163.14, and 164.19 eV, due to C-S group, and S-H group in the molecular structure of PFDT oligomer, respectively (curve B) [42, 43].

3.6. Stability and durability

The superhydrophobic rGO-PDA-PFDT membrane was exposed to air for 12 months to test its environmental stability and durability. The value of static WCA was almost unchanged, confirming that this superhydrophobic composite surface has long-term stability and durability in air atmosphere.

In addition, the stability of the as-prepared rGO-PDA-PFDT membrane in acidic and alkaline pH was also investigated. Aqueous solutions of different pH values (from 1 to 14) were prepared using hydrochloric acid or sodium hydroxide. The WCAs of all the solutions of different pH values were higher than 150°, indicating superhydrophobicity (**Fig. 11a**). Moreover, the WCAs had nearly no variation, after immersion in a hydrochloric acid solution of pH 1, a sodium hydroxide solution of pH 14, and also a sodium chloride solution of pH 7 for 24 h at room temperature, suggesting a good chemical stability of the superhydrophobic membrane (**Fig. 11b**).

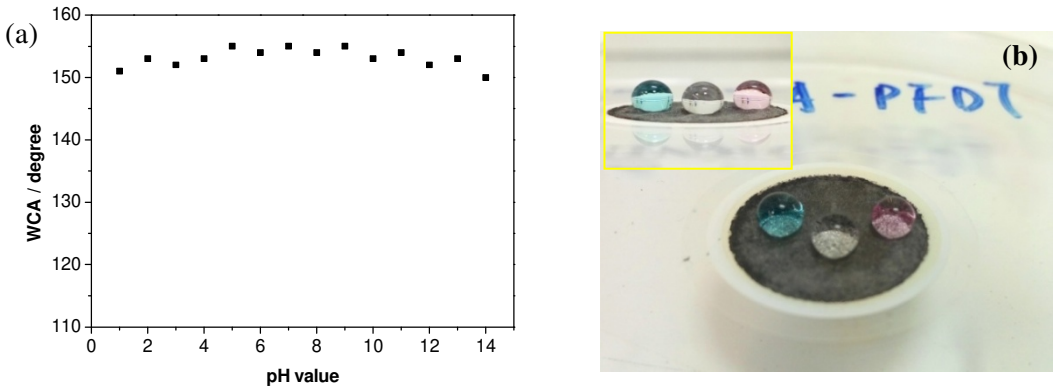

Figure 11. (a) WCAs of the SS rGO-PDA-PFDT membrane using aqueous solutions of different pH values (from 1 to 14); (b) the image of different water droplets on the superhydrophobic membrane: HCl solution of pH 1 (left, blue droplet), NaOH solution of pH 14 (right, pink droplet) and NaCl solution of pH 7 (middle, colorless).

3.7. Separation of oil from water

The surface free energy (tension) of water is commonly much greater than that of organic solvents. Therefore, solid surfaces possess the proper surface free energy (between those of water and organic solvents) such that both hydrophobicity and oleophilicity might be exhibited. Combined with an appropriate surface morphology, porous superhydrophobic-superoleophilic (SS) materials can be prepared. By combining superhydrophobicity with

superoleophilicity, a porous surface that possesses special wettability is introduced, intended to be used to separate organic solvents from water.

For water droplets (the surface tension is about 72.75 mN/m at 20 ºC), the rGO-PDA-PFDT membrane displays superhydrophobicity with a WCA of about 156º, and the water cannot permeate into the porous surface. For organic droplets, the surface exhibits superoleophilicity, and the organic solvent can quickly permeate into the membrane. Here, we recorded the contact angles of different organic solvents, such as chloroform (28.51 mN/m), hexane (18.40 mN/m), toluene (27.73 mN/m), acetone (23.70 mN/m) and 1-octane (22.60 mN/m). All of them showed superoleophilicity with CA of almost 0º. The big difference of wettability between water and organic solvents on the porous surface provides a strategy to separate mixtures of water and organic solvents effectively.

The separation experiment of water and chloroform has been realized, as graphically depicted in **Figure 12** and **video S2**. In the separation device, the as-prepared rGO-PDA-PFDT membrane was fixed to the bottom of a tube that is open at both ends (**Figure 12**).

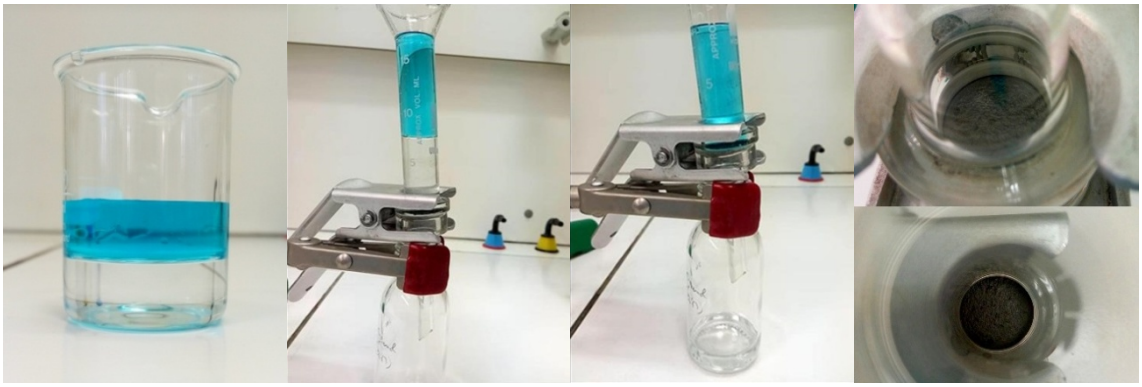

Figure 12. Photographs of the chloroform/water separation process (**video S2**). The water was dyed with Methylene Blue for clear observation.

As expected, while a mixture of water (dyed with Methylene Blue for clear observation) and chloroform was poured into the separation device, the chloroform was adsorbed and permeated through the membrane and rapidly dropped into the bottle underneath, whereas

water could not penetrate the film and still resided on the membrane. Thus, the as-prepared SS rGO-PDA-PFDT membrane can separate chloroform from water easily. In the same way, other organic solvents, such as hexane, toluene, acetone and 1-octane, can also be separated from water successfully.

To further investigate the durability and recyclability of this SS rGO-PDA-PFDT membrane, we repeated this separation process for 10 times. As expected, this SS membrane can separate chloroform form water consecutively, and the membrane surface can still maintain superhydrophobicity. **Figure 13** shows the water contact angle (WCA) of the rGO-PDA-PFDT membrane after different cycles of the separation process. Clearly, the WCA decreased only slightly from 156° to 152°, and the membrane was still superhydrophobic.

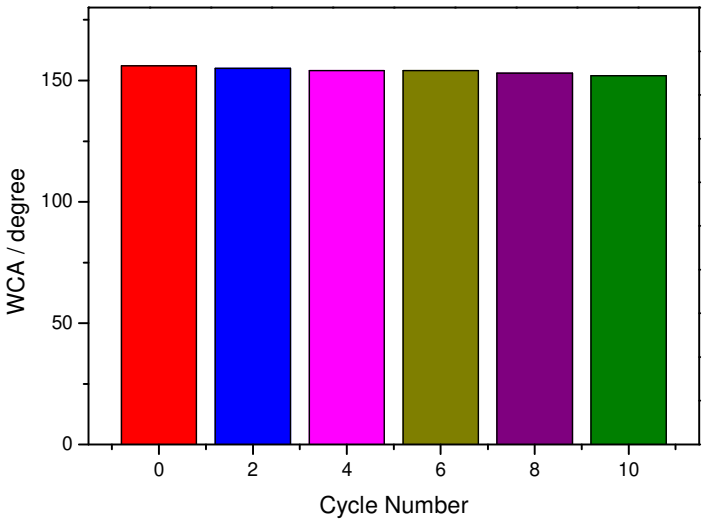

Figure 13. The WCA of the rGO-PDA-PFDT membrane after different cycles for separation process.

4. Conclusion

Superhydrophobic-superoleophilic (SS) reduced graphene oxide-polydopamine functionalized with perfluorodecanethiol (rGO-PDA-PFDT membrane) has been successfully fabricated by a facile two-steps method, taking advantage of the excellent adhesive properties of polydopamine and the low surface energy of PFDT molecules. The rGO-PDA-PFDT

membrane displayed a water contact angle (WCA) of 156º without hysteresis, indicating that the water droplet can be described by the Cassie-Baxter model. By calculation, approximately 7% acts as the contact area of the water droplet and the solid surface, and the remaining 93% serves as the contact area of the water droplet and air. The contact angles of various organic solvents (chloroform, hexane, toluene, acetone, 1-octane) were almost 0º, indicating superoleophilicity. The rGO-PDA-PFDT membrane exhibited good stability in both acidic and alkaline solutions even after 24 h immersion in these solutions. The superhydrophobic and superoleophilic properties of the rGO-PDA-PFDT membrane were successfully applied for the separation of chloroform from water. The good stability of the membrane combined with its excellent ability for separation of organic solvents from water hold promise for the development of versatile membranes for oil filtration for various applications in environmental remediation.

Acknowledgements

R.B., S.S., Y.C. and A.B. gratefully acknowledge financial support from the Centre National de la Recherche Scientifique (CNRS), the University of Lille – Sciences et Technologies, and the Hauts-de-France region. This work was partly supported by the French RENATECH network (French national nanofabrication platform). Y.C. thanks Chinese government for the China Scholarship Council Award. Y.C. gratefully acknowledges the Research Initiation Fund Project of the Ministry of Education of China (No. 2652018052) for this work.

Supporting Information

Figure S1: High resolution XPS spectra of the (a) O_{1s} and (b) N_{1s}. (A) rGO-PDA (blue line), (B) rGO-PDA-PFDT (red line). The inset of (a) is the fitted curve of sample A.

Video S1: The water droplet touches and leaves the SS surface.

Video S2: Video of the chloroform/water separation process.

References

[1] W.J. Liu, H. Jiang, H.Q. Yu, Development of Biochar-Based Functional Materials: Toward a Sustainable Platform Carbon Material, Chem. Rev. 115 (2015) 12251-12285.

[2] M.M. Titirici, R.J. White, N. Brun, V.L. Budarin, D.S. Su, F. del Monte, J.H. Clark, M.J. MacLachlan, Sustainable carbon materials, Chem. Soc. Rev. 44 (2015) 250-290.

[3] S.P. Dharupaneedi, R.V. Anjanapura, J.M. Han, T.M. Aminabhavi, Functionalized Graphene Sheets Embedded in Chitosan Nanocomposite Membranes for Ethanol and Isopropanol Dehydration via Pervaporation, Ind. Eng. Chem. Res. 53 (2014) 14474-14484.

[4] X. W. Yu, H. H. Cheng, M. Zhang, Y. Zhao, L. T. Qu, G. Q. Shi, Graphene-based smart materials, Nature Rev. Mater. 2 (2017) 17046.

[5] K. Turcheniuk, R. Boukherroub, Sabine Szunerits, Gold-graphene nanocomposites for sensing and biomedical applications, J. Mater. Chem. B 3 (2015) 4301-4324.

[6] R. Boukherroub, S. Szunerits, Graphene based biosensors, Interface Focus 8 (2018) 20160132

[7] X. Li, L. Zhi, Graphene hybridization for energy storage applications, Chem. Soc. Rev. 47 (2018) 3189-3216

[8] R. Das, C. D. Vecitis, A. Schulze, B. Cao, A. F. Ismail, X. B. Lu, J. P. Chen, S. Ramakrishna, Recent advances in nanomaterials for water protection and monitoring, Chem. Soc. Rev. 46 (2017) 6946-7020.

[9] H. Lee, S. M. Dellatore, W. M. Miller, P. B. Messersmith, Mussel-Inspired Surface Chemistry for Multifunctional Coatings, Science 318 (2007) 426–430.

[10] Q. Ye, F. Zhou, W. Liu, Bioinspired catecholic chemistry for surface modification, Chem. Soc. Rev. 40 (2011) 4244-4258.

[11] T. G. Barclay, H. M. Hegab, S. R. Clarke, M. Ginic-Markovic, Versatile Surface Modification Using Polydopamine and Related Polycatecholamines: Chemistry, Structure, and Applications, Adv. Mater. Interfaces, 4 (2017) 1601192.

[12] Y. K. Jeong, S. H. Park, J. W. Choi, Mussel-Inspired Coating and Adhesion for Rechargeable Batteries: A Review, ACS Appl. Mater. Interfaces 10 (2018) 7562-7573.

[13] R. Batul, T.a Tamanna, A. Khaliq, A. Yu, Recent progress in the biomedical applications of polydopamine nanostructures, Biomater. Sci. 5 (2017) 1204-1229.

[14] L. Q. Xu, W. J. Yang, K.-G. Neoh, E.-T. Kang, G. D. Fu, Dopamine-Induced Reduction and Functionalization of Graphene Oxide Nanosheets, Macromolecules 43 (2010) 8336-8339.

[15] Y. J. Mi, Z. F. Wang, X. H. Liu, S. R. Yang, H. G. Wang, J. F. Ou, Z. P. Li, J. Q. Wang, A simple and feasible in-situ reduction route for preparation of graphene lubricant films applied to a variety of substrates, J. Mater. Chem. 22 (2012) 8036-8042.

[16] H. Y. Liu, P. X. Xi, G. Q. Xie, Y. J. Shi, F. P. Hou, L. Huang, F. J. Chen, Z. Z. Zeng, C. W. Shao, J. Wang, Simultaneous Reduction and Surface Functionalization of Graphene Oxide for Hydroxyapatite Mineralization, J. Phys. Chem. C 116 (2012) 3334-3341.

[17] I. Kaminska, M. R. Das, Y. Coffinier, J. Niedziolka-Jonsson, J. Sobczak, P. Woisel, J. Lyskawa, M. Opallo, R. Boukherroub, S. Szunerits, Reduction and functionalization of graphene oxide sheets using biomimetic dopamine derivatives in one step, ACS Appl. Mater. Interfaces 4 (2012) 1016-1020.

[18] F. Liu, F. Sun, Q. Pan, Highly compressible and stretchable superhydrophobic coating inspired by bioadhesion of marine mussels, J. Mater. Chem. A 2 (2014) 11365-11371.

[19] N. Cao, B. Yang, A. Barras, S. Szunerits, R. Boukherroub, Polyurethane sponge functionalized with superhydrophobic nanodiamond particles for efficient oil/water separation, Chem. Eng. J. 307 (2017) 319-325.

[20] N. Cao, Q. Lyu, J. Li, Y. Wang, B. Yang, S. Szunerits, R. Boukherroub, Facile synthesis of fluorinated polydopamine/chitosan/reduced graphene oxide composite aerogel for efficient oil/water separation, Chem. Eng. J. 326 (2017) 17-28.

[21] O. Oribayo, X. Feng, G. L. Rempel, Q. Pan, Synthesis of lignin-based polyurethane/graphene oxide foam and its application as an absorbent for oil spill clean-ups and recovery, Chem. Eng. J. 323 (2017) 191-202.

[22] M. Peng, Y. Zhu, H. Li, K. He, G. Zeng, A. Chen, Z. Huang, T. Huang, L. Yuan, G. Chen, Synthesis and application of modified commercial sponges for oil-water separation, Chem. Eng. J. 373 (2019) 213-226.

[23] J. Wang, J.X.H. Wong, H. Kwok, X. Li, H.-Z. Yu, Facile Preparation of Nanostructured, Superhydrophobic Filter Paper for Efficient Water/Oil Separation, PLOS ONE 11 (2016) e0151439.

[24] D.P. Suhas, T.M. Aminabhavi, H.M. Jeong, A.V. Raghu, Hydrogen peroxide treated graphene as an effective nanosheet filler for separation application, RSC Adv. 5 (2015) 100984-100995.

[25] O. Fellahi, M.R. Das, Y. Coffinier, S. Szunerits, T. Hadjersi, M. Maamache, R. Boukherroub, Silicon nanowire arrays-induced graphene oxide reduction under UV irradiation, Nanoscale 3 (2011) 4662-4669.

[26] R.N. Wenzel, Resistance of solid surfaces to wetting by water, Ind. Eng. Chem. 28 (1936) 988-994.

[27] A.B.D. Cassie, S. Baxter, Wettability of porous surfaces, Trans. Faraday Soc. 40 (1944) 0546-0550.

[28] I. Kaminska, W. Qi, A. Barras, J. Sobczak, J. Niedziolka-Jonsson, P. Woisel, J. Lyskawa, W. Laure, M. Opallo, M. Li, R. Boukherroub, S. Szunerits, Thiol–yne click reactions on alkynyl–dopamine-modified reduced graphene oxide, Chem. Eur. J. 19 (2013) 8673-8678.

[29] D. Zhong, Q.L. Yang, L. Guo, S.X. Dou, K.S. Liu, L. Jiang, Fusion of nacre, mussel, and lotus leaf: bio-inspired graphene composite paper with multifunctional integration, Nanoscale 5 (2013) 5758-5764.

[30] I. Kaminska, M.R. Das, Y. Coffinier, J. Niedziolka-Jonsson, J. Sobczak, P. Woisel, J. Lyskawa, M. Opallo, R. Boukherroub, S. Szunerits, Reduction and Functionalization of Graphene Oxide Sheets Using Biomimetic Dopamine Derivatives in One Step, ACS Appl. Mater. Interfaces 4 (2012) 1016-1020.

[31] Y.J. Mi, Z.F. Wang, X.H. Liu, S.R. Yang, H.G. Wang, J.F. Ou, Z.P. Li, J.Q. Wang, A simple and feasible in-situ reduction route for preparation of graphene lubricant films applied to a variety of substrates, J. Mater. Chem. 22 (2012) 8036-8042.

[32] S.A. Centeno, J. Shamir, Surface enhanced Raman scattering (SERS) and FTIR characterization of the sepia melanin pigment used in works of art, J. Mol. Struct. 873 (2008) 149-159.

[33] R.A. Zangmeister, T.A. Morris, M.J. Tarlov, Characterization of Polydopamine Thin Films Deposited at Short Times by Autoxidation of Dopamine, Langmuir 29 (2013) 8619-8628.

[34] A.V. Raghu, G.S. Gadaginamath, N.T. Mathew, S.B. Halligudi, T.M. Aminabhavi, Synthesis and characterization of novel polyurethanes based on 4,4′-[1,4-phenylenedi-

diazene-2,1-diyl]bis(2-carboxyphenol) and 4,4′-[1,4-phenylenedi-diazene-2,1-diyl]bis(2-chlorophenol) hard segments, Reactive Funct. Polym. 67 (2007) 503-514.

[35] A.V. Raghu, G.S. Gadaginamath, H.M. Jeong, N.T. Mathew, S.B. Halligudi, T.M. Aminabhavi, Synthesis and characterization of novel Schiff base polyurethanes, J. Appl. Polym. Sci. 113 (2009) 2747-2754.

[36] H.L. Wang, J.T. Robinson, X.L. Li, H.J. Dai, Solvothermal Reduction of Chemically Exfoliated Graphene Sheets, J. Am. Chem. Soc. 131 (2009) 9910.

[37] R.P. Gu, W.Z. Xu, P.A. Charpentier, Synthesis of polydopamine-coated graphene-polymer nanocomposites via RAFT polymerization, J. Polym. Sci. Pol. Chem. 51 (2013) 3941-3949.

[38] J.F. Ou, L. Liu, J.Q. Wang, F.J. Wang, M.S. Xue, W. Li, Fabrication and Tribological Investigation of a Novel Hydrophobic Polydopamine/Graphene Oxide Multilayer Film, Tribol. Lett. 48 (2012) 407-415.

[39] Y.F. Mo, M. Zhu, M.W. Bai, Preparation and nano/microtribological properties of perfluorododecanoic acid (PFDA)-3-aminopropyltriethoxysilane (APS) self-assembled dual-layer film deposited on silicon, Colloid Surf. A 322 (2008) 170-176.

[40] S.J.R. Prabakar, Y.H. Hwang, E.G. Bae, S. Shim, D. Kim, M.S. Lah, K.S. Sohn, M. Pyo, SnO2/Graphene Composites with Self-Assembled Alternating Oxide and Amine Layers for High Li-Storage and Excellent Stability, Adv. Mater. 25 (2013) 3307-3312.

[41] L.J. Yan, X.J. Bo, D.X. Zhu, L.P. Guo, Well-dispersed Pt nanoparticles on polydopamine-coated ordered mesoporous carbons and their electrocatalytic application, Talanta 120 (2014) 304-311.

[42] H. Qian, M. Li, Z. Li, Y. Lou, L. Huang, D. Zhang, D. Xu, C. Du, L. Lu, J. Gao, Mussel-inspired superhydrophobic surfaces with enhanced corrosion resistance and dual-action antibacterial properties, Mater. Sci. Eng. C 80 (2017) 566-577.

[43] Y. Ge, J.E. Whitten, Interfacial electronic properties of thiophene and sexithiophene adsorbed on a fluorinated alkanethiol monolayer, J. Phys. Chem. C 112 (2008) 1174-1182.

Graphical Abstract

Stable superhydrophobic/superoleophilic rGO-PDA-PFDT membrane has been fabricated by facile and simple method for oil/water separation.